



# Preoperative prediction of lymphovascular invasion and T-staging of rectal cancer via a dual-energy computed tomography iodine map: a feasibility study

Jinliang Zhang<sup>1\*</sup>

Hui Qi<sup>2\*</sup>

Chun Yang<sup>2</sup>

Ling Liu<sup>3</sup>

Yuxin Wang<sup>2</sup>

Wei Li<sup>2</sup>

<sup>1</sup>Shandong Public Health Clinical Center, Department of Medical Imaging, Jinan, China

<sup>2</sup>The First Affiliated Hospital of Shandong First Medical University, Department of Medical Imaging, Jinan, China

<sup>3</sup>GE Healthcare, CT Imaging Research Center, Shanghai, China

\*Joint first authors

Corresponding author: Wei Li

E-mail: lwqfsh@126.com

Received 11 March 2024; revision requested 16 April 2024; accepted 12 May 2024.



Epub: 05.06.2024

Publication date: 30.12.2024

DOI: 10.4274/dir.2024.242755

## PURPOSE

To investigate the value of dual-energy computed tomography (DECT) in predicting lymphovascular invasion (LVI) and the accuracy of preoperative T-staging of rectal cancer (RC).

## METHODS

Forty-nine patients with RC who had not received radiotherapy were enrolled to undergo a DECT scan. All patients underwent surgical tumor resection within 3–5 days after the DECT scan. Preoperative T-staging of RC based on images was performed by experienced radiologists. The normalized iodine concentrations (NIC) of the tumor and the perirectal adipose tissue (PAT) from the arterial phase (AP) and venous phase (VP) were measured using DECT. The tumor LVI and T-staging confirmed by pathology were used as the gold standard for grouping (group A, LVI–; group B, LVI+; group C, T1–2; and group D, T3–4a). The NIC values between two groups were compared using the Mann–Whitney U test, with  $P < 0.05$  indicating a statistically significant difference. The accuracy of NIC in predicting LVI and distinguishing T1–2 RC from T3–4a RC were determined via receiver operating characteristic curve analysis, and the optimal cut-off of NIC was determined using the area under the curve.

## RESULTS

The tumor NIC values were significantly higher in the LV+ group than in the LVI– group in the VP ( $0.728 \pm 0.031$  vs.  $0.669 \pm 0.034$ ,  $P < 0.001$ ). The NIC values of PAT were significantly higher in the T3–4a group than in the T1–2 group in both the AP ( $4.034 \pm 0.991$  vs.  $3.115 \pm 0.581$ ,  $P < 0.05$ ) and the VP ( $5.481 \pm 1.054$  vs.  $3.450 \pm 0.980$ ,  $P < 0.001$ ). The accuracy of using NIC values to distinguish between the LVI+ group and the LVI– group and to diagnose the T3–4a group were 85.7% and 89.8%, respectively. However, there was no statistically significant difference between the NIC value in the LVI+ group and in the LVI– group in the AP. There was also no statistical difference in the tumor NIC value between the T1–2 group and the T3–4a group.

## CONCLUSION

The tumor and PAT NIC are valuable indicators in RC that can preoperatively predict LVI and improve the accuracy of preoperative RC T-staging.

## CLINICAL SIGNIFICANCE

The use of DECT improves the T-staging and LVI prediction of RC, which is helpful in guiding the clinical selection of appropriate treatment modalities and improving prognostic outcomes.

## KEYWORDS

DECT, lymphovascular invasion, normalized iodine concentration, rectal cancer, T-staging

According to the 2022 global cancer statistics, rectal cancer (RC) is the third most common malignant cause of morbidity (19.5%) and mortality (9.0%) and has become a major global health problem.<sup>1</sup> Preoperative staging of patients using imaging instruments has a great clinical significance for formulating the best possible individualized treatment plan.<sup>2</sup> Currently, TNM staging is globally recognized as a standard staging system for distinguishing the extent of cancer spread. The T-stages of RC according to the 8<sup>th</sup> edition of the cancer staging manual<sup>3</sup> are shown in Table 1. This staging system has a notable clinical significance for preoperatively distinguishing between stage T1-2 RC and stage T3-4 RC,<sup>4</sup> and relevant research shows that patients with T1-2 RC have a low recurrence rate after radical surgery, which can effectively prolong the survival period; in contrast, patients with T3-4 RC do not directly benefit from surgery, and preoperative adjuvant radiotherapy and chemotherapy are needed to improve the surgical resection and radical cure rate.<sup>5</sup> Whether there is lymphovascular invasion (LVI) can be a decidable indicator of preoperative adjuvant chemotherapy.<sup>6</sup> For patients with stage T3-4 or LVI+ RC, declining the adenocarcinoma grade before surgery is significant for treatment and prognosis.<sup>1,7</sup>

Transrectal ultrasonography (TRUS) and magnetic resonance imaging (MRI) have been widely used for preoperative T-staging of RC, and the diagnostic accuracies of TRUS for preoperative T-staging of patients with RC have been reported in the literature to range from 71% to 95%.<sup>8</sup> However, the diagnostic accuracy of TRUS is highly dependent on the experience and skill of the operator.<sup>9</sup> Moreover, the field of view of TRUS is limited,

and high-grade and stenotic tumors are often difficult to reach with the probe.<sup>10</sup> Preoperative T-staging of patients with RC via MRI has been proven to have an accuracy of 65%–86%, and MRI has become the most commonly used technology in clinical rectal examination.<sup>11,12</sup> However, despite the many advantages of the radiation-free rectal MRI, the examination is expensive, requires a long scanning time and presents a potential safety risk for some specific individuals (e.g., those with metal implants, claustrophobia, and epilepsy).<sup>13</sup> In addition, the preparation for patients with RC is challenging (e.g., the gas and fluid in the intestines and other intestinal contents present during the examination produce artifacts on MRI images). The main advantages of computed tomography (CT) when compared with MRI are more available clinical scanning and a shorter scanning time; thus, CT is often used to detect distant metastases in patients with RC. In clinical practice, radiologists also use conventional CT to complete preoperative-image naked-eye T-staging of RC. Some studies<sup>12,14</sup> note that it is difficult to precisely distinguish stage T2 RC and T3 RC using CT or MRI images, since the rectal surface is rough, and the indication of peripheral fat is uneven. Therefore, determining whether the condition is caused by tumor infiltration from only the imaging point of view is complicated. Moreover, inflammatory exudation is easily misdiagnosed as a fibrous cord of adipose tissue around the RC in cancer invasion, causing a high false positive rate for clinical diagnosis of stage T3 RC. Similarly, the appearance of a tumor invading the surrounding soft tissue is difficult to distinguish from blood vessels or local inflammation, often leading to radiologists misdiagnosing stage T3 RC as stage T2 RC. Sometimes, inflammation, image artifacts, small blood vessels, and other factors may also lead to the same imaging results. As a result, the rate of misdiagnosing stage T2 RC as stage T3 RC in clinical practice is high.

In summary, novel methods for improving the sensitivity, specificity, and accuracy of preoperative prediction of LVI and T-staging of RC are in high demand.

Dual-energy computed tomography (DECT) uses two X-ray beams of different energy levels to simultaneously scan the desired object, showing both alterations in conventional CT features and quantitatively reflecting differences in the energetic categories of tissues, thus providing many quantitative parameters reflecting biological properties, such as iodine concentration (IC).<sup>15</sup> The iodine-based images provided by DECT are pseudo-color images.<sup>16,17</sup> Compared with the images provided by conventional CT, which only provide a CT value, DECT iodine-based images are more convenient for naked-eye distinguishing of the RC invasion extent. In addition, the IC provided by DECT is a quantitative parameter that can provide a better objective basis for diagnosis. For early invasion of cancer cells, abnormal tumor angiogenesis appears in the affected area, and DECT can evaluate the microcirculation in the region of interest (ROI) by measuring the concentration of iodine in the adipose tissue around the tumor, thus helping determine whether it has been invaded.<sup>18,19</sup> Furthermore, DECT can detect the iodine density maps in the tissue, since it can simultaneously collect two data sets of different energy spectra in a single acquisition, and iodine has strong photoelectric absorption at the low tube voltage close to the K edge of iodine, making it easily distinguishable from other materials.<sup>18</sup> Related studies have shown that IC in perigastric adipose tissue can predict whether gastric cancer will invade the serosa tissue and determine the T4 stage of gastric cancer.<sup>20</sup> Moreover, DECT has been used to identify various other diseases (e.g., lymph node metastasis of colorectal cancer,<sup>21,22</sup> liver metastasis of colorectal cancer<sup>23-25</sup>) and determine the diagnostic classi-

#### Main points

- Preoperative prediction of lymphovascular invasion (LVI) and T-staging of rectal cancer (RC) via a dual-energy computed tomography (DECT) iodine map.
- Compared with the pathological gold standard, the accuracy of conventional computed tomography in differentiating between T3-4a RC and T1-2 RC was only 67.3%, whereas the accuracy of iodine mapping using DECT was 89.8%. In addition, DECT was relatively effective in predicting LVI positivity (85.7%).
- The obtained results showed that the normalized iodine concentration of the tumor and the perirectal adipose tissue in RC can preoperatively predict LVI and improve the accuracy of T-staging.

**Table 1.** T-staging for rectal cancer

| T-staging | Rectal wall involvement/description   |  |
|-----------|---|--|
| T0        | No evidence of primary tumor  |  |
| Tis       | Carcinoma <i>in situ</i> , intramucosal (tumor invades the <i>lamina propria</i> of the mucosa but does not break through the muscular layer of the mucosa) |  |
| T1        | Tumor invasion of the submucosa   |  |
| T2        | Tumor invasion of the <i>lamina propria</i>   |  |
| T3        | Tumor penetration of the intrinsic muscular layer to reach the subplasma layer or invasion of paracolorectal tissue without peritoneal coverage             |  |
| T4        | T4a   | Tumor penetration of the peritoneal visceral layer                 |
|           | T4b   | Tumor directly invades or adheres to adjacent organs or structures |

fication of benign and malignant colorectal lymph nodules.<sup>26</sup> Thus, this study aims to evaluate the value of IC in RC PAT and tumors using DECT in predicting (i) pre-operative LVI and (ii) the accuracy of preoperative RC T-staging.

## Methods

### Patient characteristics

The study was approved according to the principles of the Declaration of Helsinki by the Local Institutional Ethics Committee of the First Affiliated Hospital of Shandong First Medical University [approval no: 2022 LUN (S521)], and all participants signed a written informed consent form. A total of 62 patients with non-T4b-stage primary RC endoscopically and pathologically confirmed between November 2020 and February 2022 were retrospectively enrolled in the study. The 62 patients underwent preoperative DECT scanning at the First Affiliated Hospital of Shandong First Medical University. All enrolled patients underwent three-phase DECT scans, including unenhanced CT scan and contrast-enhanced arterial phase (AP) and venous phase (VP) DECT scans.

Of the 62 patients initially included in the study, 13 were excluded (2 without adequate intestinal preparation, 2 who underwent surgery more than a week after the CT scan, 3 with severe image artifacts, 4 who refused to accept any treatment, and 2 who underwent preoperative neoadjuvant chemotherapy). A

final number of 49 subjects was selected (33 men and 16 women), with an average age of 61.3 years (31–76 years). The inclusion and exclusion criteria are summarized in Figure 1, and the patient characteristics are shown in Table 2.

The surgically resected tissue specimens were pathologically examined and utilized as the gold standard to determine the RC stage. Some studies stage-divided RC into the T1-2 group and the T3-4 group based on prognosis.<sup>27,28</sup> Considering that the T4b stage could be clearly differentiated from the T3 stage on CT images, all enrolled patients with stage T4 RC indicated stage T4a RC. Finally, the patients were divided into group A (LVI-) and group B (LVI+); group C (no serosa invasion, T1-2), and group D (serosa invasion, T3-4a).

### Dual-energy computed tomography scan

All DECT images were acquired using a 256-row energy spectrum CT scanner (Revolution CT, GE Healthcare, WI, USA). An intestine preparation time of 30 minutes was required per patient before the CT examination. A mixture of pure water and medical ultrasonic couplants at a ratio of 1:1 was prepared and injected into the rectum based on the distance between the tumor and the anus. Moreover, 400 mL of water was given to patients before the DECT examination.

All patients received routine intravenous administration, followed by an intravenous injection of the contrast agent, iopromide

(370 mg iodine/mL, Ultravist®, Bayer Schering Pharma), through the elbow vein at a flow rate of 4 mL/s. The injection dose of the contrast agent was calculated based on the body weight (2 mL/kg) of each patient. The scanning of the AP was triggered at a threshold of 100 HU for the abdominal aorta. After a delay of 40 seconds, VP scanning was performed. Thus, DECT images in the AP and VP were achieved.

The conventional imaging acquisition protocol was as follows: tube voltage = 120 kVp; automatic tube current modulation range = 200–720 mA; noise index (NI) = 10; rotation time = 0.8 s; detector coverage = 80 mm; scan slice thickness = 5 mm; reconstructed thickness/interval = 0.625/0.625 mm; and pitch = 0.992:1. The spectral (Gemstone Spectral Imaging) mode was used in both the AP and VP using the following parameters: tube voltage = 80 and 140 kVp with a tin filter; tube currents = 190 mA; NI = 10; rotation time = 0.8 s; detector coverage = 80 mm; scan slice thickness = 5 mm; reconstructed thickness/interval = 0.625/0.625 mm; and pitch = 0.992:1.

### Image analysis and quantitative parameters

Two experienced radiologists performed naked-eye preoperative T-staging of patients with RC using a PACS system and conventional CT images, as shown in Figure 2, Figure 3a and b. The staging was as follows: (1) T1-2 stage: the tumor had invaded the

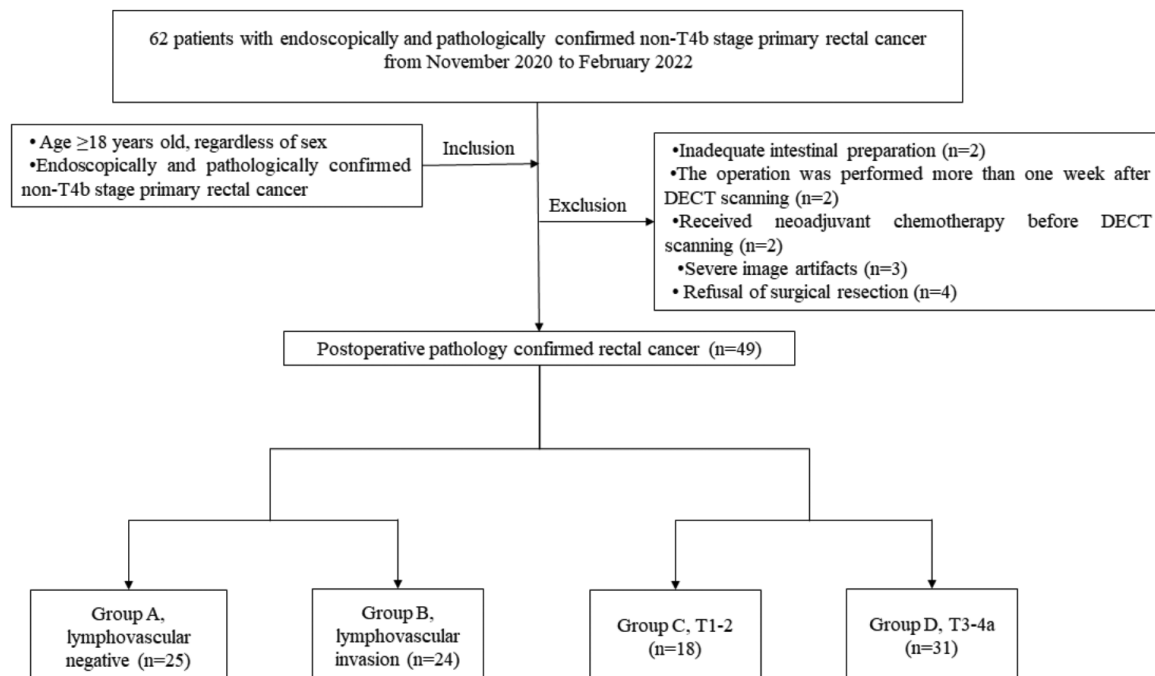


Figure 1. Flowchart showing the inclusion and exclusion criteria for patient selection. DECT, dual-energy computed tomography.

submucosal and muscular layers but had not breached the muscularis propria; (2) T3 stage: the tumor had penetrated the intrinsic muscle layer and reached the lower serosa layer or invaded the perirectal tissue without peritoneal coating; (3) and T4 stage: the tumor had penetrated the serous layer and reached the peritoneum (T4a), or adjacent organs were involved (T4b). Morphological features included plain scan and enhanced scan CT values, whether the tumor edge was blurred, whether the density of adjacent adipose tissue had increased, and whether the surrounding structures and organs had been infiltrated. The radiologists were blinded to the results of IC measurement and histology.

A slice thickness of 0.625 mm was chosen to reconstruct the dual-energy AP and VP iodine-based images to quantitatively measure IC using a GE AW4.2 workstation (GE Healthcare). The IC was calculated by manually delineating ROIs in the tumor, perirectal adipose tissue (PAT), and iliac arteries. A 50–75 mm<sup>2</sup> ROI was obtained from the tumor and iliac artery, covering as much tumor as possible, outside of blood vessels and necrotic lesions. A 45–70 mm<sup>2</sup> ROI was found in

the PAT; the distance between the ROI and RC intestinal wall was >1 mm, and the ROI didn't involve the tumor intestinal wall.<sup>20</sup> To obtain the adipose tissue normalized IC (NIC), identical ROIs of the same size were placed at the same level in the area away from the tumor (Figure 2, Figure 3c-f).

The corresponding IC was measured from the AP and VP images of each patient. Each measurement was repeated six times (three layers of images were selected for measurement, and the data from each layer were measured twice), and the average IC was recorded for further analysis. The second measurement was completed using the same method after 2 months, and the two measuring results were averaged to obtain more rigorous measurement results.

The NIC<sub>1</sub> values of the initial lesion and the NIC<sub>2</sub> values of the adipose tissue around the RC were calculated using the following formulas:  $NIC_1 = \frac{IC_{tumor}}{IC_{iliac\ artery}}$ ,  $NIC_2 = \frac{IC_{near\ the\ RC}}{IC_{away\ from\ RC}}$ , which minimized variations in different patients.

### Statistical analysis

Statistical analysis was performed using the SPSS 26.0 software (IBM Corp. Armonk,

NY, USA). The Mann–Whitney U test was used to compare the NIC values between group A and group B;  $P < 0.05$  was considered statistically significant. The values of NIC<sub>1</sub> and NIC<sub>2</sub> in diagnosing LVI and T3-4a RC were determined via receiver operating characteristic (ROC) curve analysis. The area under the ROC curve (AUC) was used to determine the optimal cut-off of NIC for tumor classification. Inter-observer agreement between two measurements of DECT parameters was evaluated using the interclass correlation coefficient (ICC). The ICC values were as follows: <0.5 = poor reliability; 0.5–0.75 = moderate reliability, 0.75–0.9 = good reliability; and >0.9 = excellent reliability.

## Results

### Quantitative parameters of dual-energy computed tomography

In the AP, the difference in the NIC<sub>1</sub> values between group A and group B was not statistically significant ( $P > 0.05$ ). However, in the VP, the NIC<sub>1</sub> was significantly higher in group B than in group A ( $0.728 \pm 0.031$  vs.  $0.669 \pm 0.034$ ,  $P < 0.001$ ) (Table 2). For VP images, the ROC curve (Figure 4) analysis of LVI pre-

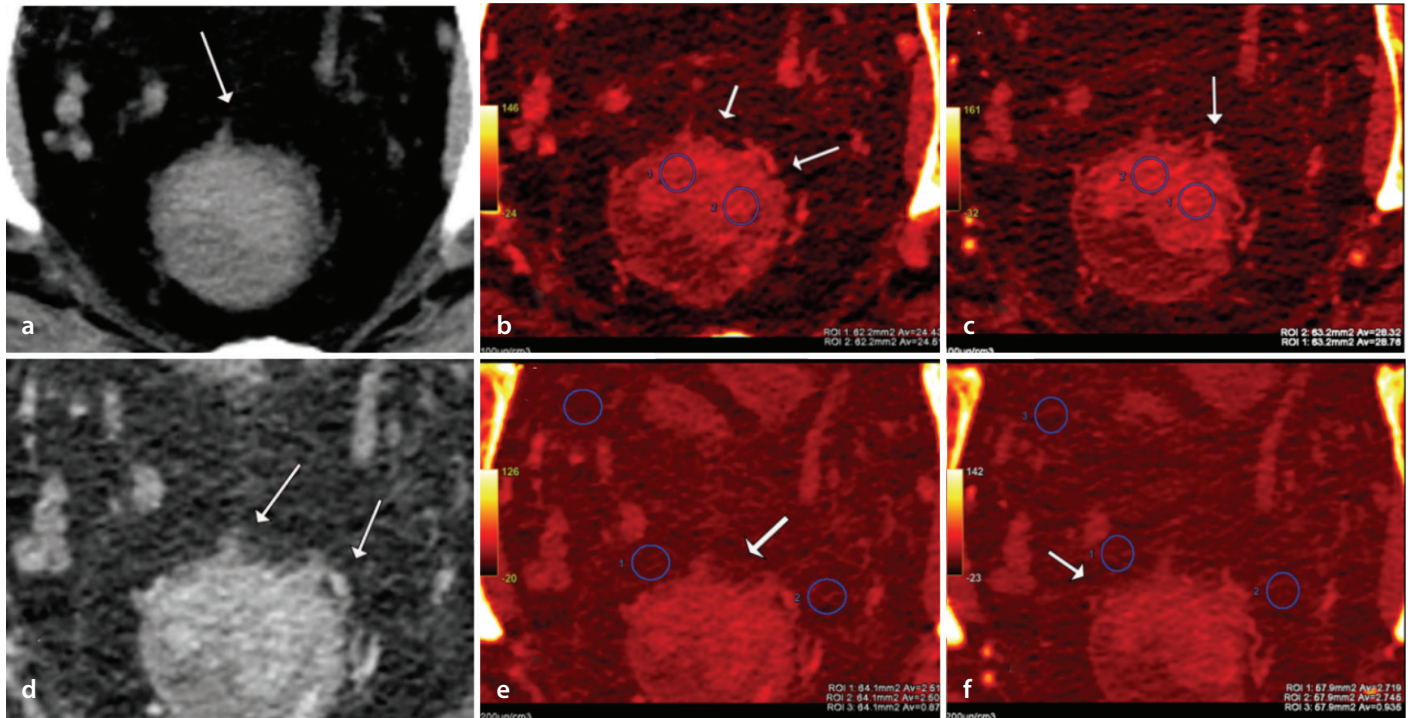


**Figure 2.** A 60-year-old man with lymphovascular invasion negative stage T2 rectal cancer. The white arrow denotes the thickening and transmural enhancement of the rectal wall. The density of the perirectal fat increases with the stripe-like shadow. In (a) and (b), the radiologist diagnosed the rectal tumor as clinical staging T3 with traditional computed tomography (CT) before surgery, but the pathological stage was pathological staging T2; (c-f) were used to measure the iodine concentration (IC) in tissues using post-processing techniques; (c) and (d) show the method of drawing regions of interest (ROIs) on the tumor in the arterial phase (AP) and venous phase (VP), respectively; (e) shows that the mean IC was 0.501 mg/mL in the perirectal fat tissue (ROI: 1.2) and 0.175 mg/mL in the fat tissue distant from the tumor in the AP (ROI: 3); (f) shows that the mean IC was 0.546 mg/mL in the fat tissue near the tumor (ROI: 1.2), and 0.195 mg/mL in the fat tissue distant from the tumor in the VP (ROI: 3). The dual-energy CT corrected the preoperative T-staging of the patient as non-T3.

diction via DECT denoted that the AUC was 0.868, and the best cut-off of  $NIC_1$  for distinguishing group B from group A was 0.690, with a sensitivity of 87.5%, a specificity of 84.0%, and an accuracy of 85.7%.

There was no statistical difference in the tumor  $NIC_1$  values between group C and group D. However, the  $NIC_2$  was significantly higher in group D than in group C in both the AP ( $4.034 \pm 0.991$  vs.  $3.115 \pm 0.581$ ,  $P < 0.05$ ) and the VP ( $5.481 \pm 1.054$  vs.  $3.450 \pm 0.980$ ,  $P < 0.001$ ) (Table 2). The ROC curve (Figure 5) analysis of the preoperative T-staging of RC showed that the AUC was 0.794 in the AP image and 0.905 in the VP image. For AP images, the best cut-off of  $NIC_2$  for distinguishing group D from group C was 3.346, with a sensitivity of 80.6%, a specificity of 77.3%, and an accuracy of 83.7%. The best cut-off of  $NIC_2$  for the VP image was 4.105, with a sensitivity of 90.3%, specificity of 88.9%, and accuracy of 89.8%.

#### Interobserver agreement for dual-energy computed tomography spectral parameters

The ICC score of  $NIC_1$  was 0.988 (95% CI: 0.982 to 0.992), and the ICC score of  $NIC_2$  was

0.968 (95% CI: 0.955 to 0.978), which was considered an excellent consensus.

#### Conventional computed tomography preoperative T-staging

Using the pathological results as the gold standard, 20 cases of T1-2 were diagnosed via conventional CT imaging, of which 11 cases were correctly diagnosed, and 9 cases of T3-4a were misdiagnosed as T1-2. A total of 29 patients were diagnosed with T3-4a using conventional CT imaging, of which 22 patients were correctly diagnosed, and 7 patients with T1-2 were misdiagnosed with T3-4a (Table 3). Compared with the pathological staging, the accuracy of conventional CT in differentiating T3-4a from T1-2 was 67.3% (33/49).

#### Quantitative parameters of dual-energy computed tomography T-staging

According to  $NIC$  measured by DECT, 18 patients were diagnosed with T1-2, and 31 patients were diagnosed with T3-4a in the AP. Compared with the pathological results, 14 patients were correctly diagnosed with T1-2, 4 patients with T3-4a were misdiagnosed with T1-2, 27 patients were correctly

diagnosed with T3-4a, and 4 patients with T1-2 were misdiagnosed with T3-4a (Table 3). The accuracy of DECT in differentiating T3-4a from T1-2 was 83.7% (41/49) in the AP.

In the VP, 17 patients were diagnosed with T1-2 and 32 patients with T3-4. Compared with the pathological results, 15 patients were correctly diagnosed with T1-2, 2 patients with T3-4 were misdiagnosed with T1-2, 29 patients were correctly diagnosed with T3-4, and 3 patients with T1-2 were misdiagnosed with T3-4 (Table 3). The accuracy of DECT in differentiating T3-4a from T1-2 was 89.8% (44/49) in the VP.

## Discussion

The purpose of this study was to investigate the value of DECT in predicting LVI and evaluate the accuracy of preoperative RC T-staging. The postoperative histological results were used as the gold standard for grouping.

1. The tumors were divided into the LVI- (group A) and the LVI+ (group B). The LVI was defined as the presence of cancer cells in peritumoral lymphatic vessels and small non-muscularized blood vessels or

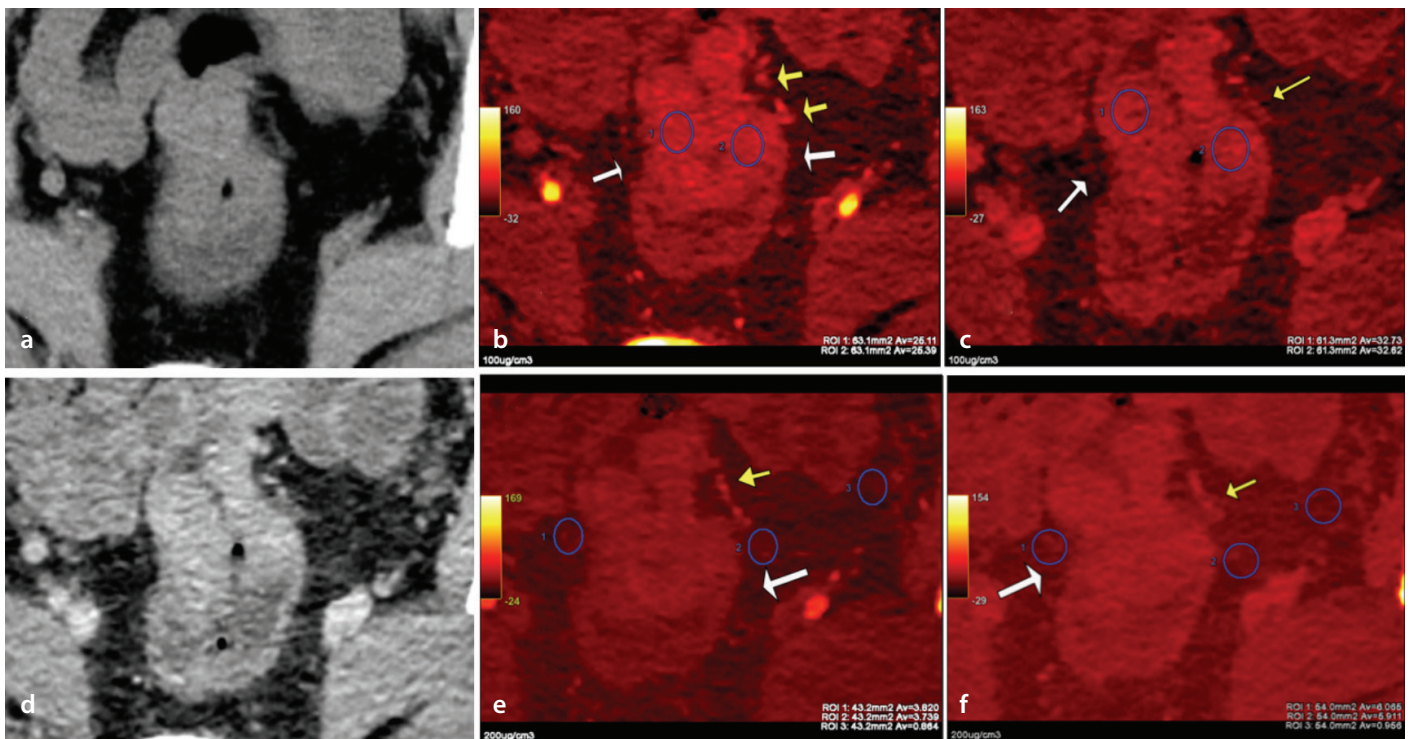


**Figure 3.** A 59-year-old man with lymphovascular invasion positive stage T3 rectal cancer. The white arrow denotes the thickening of the rectal wall, which was enhanced. The density of fat tissue around the tumor was more uniform. The local strip high-density shadow (denoted by the yellow arrow) is the vascular tissue. In (a) and (b), the radiologist diagnosed the rectal tumor as clinical staging T2 with traditional computed tomography (CT) before surgery, but the pathological stage was pathological staging T3; (c) and (d) show the method of drawing regions of interest (ROIs) on the tumor tissue in the arterial phase (AP) and the venous phase (VP), respectively; (e) shows that the mean iodine concentration (IC) was 0.756 mg/mL in the perirectal fat tissue (ROI: 1.2) and 0.173 mg/mL in the fat tissue distant from the tumor in the AP (ROI: 3); (f) shows that the mean IC was 1.198 mg/mL in the fat tissue near the tumor (ROI: 1.2), and 0.191 mg/mL in the fat tissue distant from the tumor in the VP (ROI: 3). The dual-energy CT corrected the preoperative T-staging of the patient as non-T2.

both,<sup>29</sup> and was related to the dissemination of cancer cells.<sup>30</sup> Therefore, the NIC<sub>2</sub> of the adipose tissue around the tumor was not employed to evaluate LVI. Moreover, the study found that the difference in NIC<sub>1</sub> values between group A and group B was not statistically significant ( $P > 0.05$ ) in the AP. However, in the VP, the NIC<sub>1</sub> was significantly higher in group B than in group A ( $P < 0.001$ ). Setting 0.690 as the cut-off value,

the accuracy of NIC<sub>1</sub> in LVI evaluation was 83.7%. There are several possible reasons for this result. First, LVI denoted a high invasiveness of cancer cells.<sup>31</sup> Second, the cancer cells of patients with LVI+ RC were relatively active, and the blood flow led to an increase in IC values. The study indicates that using the NIC value in the VP can distinguish between LVI- and LVI+. Further study, such as the use of a combination

of different quantitative parameters, may improve the sensitivity and specificity of DECT technology.

2. The tumors were divided into two groups: group C (no serosa invasion, T1-2) and group D (serosa invasion, T3-4a). Conventional CT scanning was used for naked-eye observation of PAT density to determine whether the serosa had been infiltrated. Seven patients with stage T1-2 RC were overestimated as having stage T3 RC, and 9 patients with stage T3 RC were underestimated as having stage T1-2 RC, with an accuracy rate of 67.3%. These findings denoted the limitations of multi-slice spiral CT in the assessment of serosa invasion. The present study demonstrated that DECT was more valuable than conventional plain CT in diagnosing T3-4a RC. The NIC<sub>2</sub> in the PAT was significantly higher when the serosa had been invaded than when it had not been invaded. The ROC curve (Figure 5) analysis showed that the NIC<sub>2</sub> was more capable of distinguishing whether RC had invaded the surrounding adipose tissue in the VP than in the AP. The accuracy of NIC<sub>2</sub> in evaluating serous infiltration was 83.7% (AP) and 89.8% (VP) when setting the cut-off as 3.346 and 4.105 in the AP and VP, respectively, which was higher than the CT value. This study found that the NIC<sub>1</sub> of RC tissue was not related to the T-stage, which differed from the results of Li et al.<sup>27</sup> A possible reason for this result is that the invasiveness of the tumor was not only related to benignancy and malignancy, but also closely related to the accuracy of cancer detection time.<sup>32</sup>

Poorly differentiated RC may not break through the muscular layer in the early stage; in contrast, highly differentiated RC may invade the peripheral adipose space of the intestinal wall; and even distant metastasis will occur in the late stage. Whether the tumor had invaded the perirectal tissue or not was the criterion for judging stage T3 of RC. In summary, these observations suggest that DECT is an innovative and accurate imaging

**Table 2.** Demographic and clinical characteristics of the included participants

| Characteristic                 | Group A (LVI-)        | Group B (LVI+)         | P value        |
|--------------------------------|-----------------------|------------------------|----------------|
| <b>Gender (n)</b>              |                       |                        |                |
| Male                           | 14                    | 19                     | 0.086          |
| Female                         | 11                    | 5                      |                |
| Age (year, mean ± SD)          | 59.7 ± 9.7            | 63.0 ± 8.7             | 0.237          |
| Height (cm)                    | 166.6 ± 6.2           | 169.6 ± 6.0            | 0.091          |
| Weight (kg)                    | 69.7 ± 8.3            | 74.4 ± 10.3            | 0.090          |
| BMI (kg/m <sup>2</sup> )       | 25.0 ± 1.8            | 25.7 ± 2.3             | 0.262          |
| <b>Quantitative parameters</b> |                       |                        |                |
| NIC <sub>1</sub> AP            | 0.126 ± 0.003         | 0.127 ± 0.005          | 0.659          |
| NIC <sub>1</sub> VP            | 0.669 ± 0.034         | 0.728 ± 0.031          | <0.001**       |
|                                | <b>Group C (T1-2)</b> | <b>Group D (T3-4a)</b> | <b>P value</b> |
| <b>Gender (n)</b>              |                       |                        |                |
| Male                           | 10                    | 23                     | 0.187          |
| Female                         | 8                     | 8                      |                |
| Age (mean ± SD)                | 59.1 ± 7.6            | 62.6 ± 9.9             | 0.065          |
| Height (cm)                    | 166.1 ± 5.6           | 169.2 ± 6.4            | 0.092          |
| Weight (kg)                    | 68.1 ± 7.8            | 74.3 ± 9.8             | 0.029*         |
| BMI (kg/m <sup>2</sup> )       | 24.6 ± 1.3            | 25.8 ± 2.3             | 0.022*         |
| <b>Stage (n)</b>               |                       |                        |                |
| T1                             | 2                     | 0                      |                |
| T2                             | 16                    | 0                      |                |
| T3                             | 0                     | 28                     |                |
| T4a                            | 0                     | 3                      |                |
| <b>Quantitative parameters</b> |                       |                        |                |
| NIC <sub>1</sub> AP            | 0.124 ± 0.003         | 0.127 ± 0.004          | 0.417          |
| NIC <sub>1</sub> VP            | 0.690 ± 0.040         | 0.704 ± 0.044          | 0.342          |
| NIC <sub>2</sub> AP            | 3.115 ± 0.581         | 4.034 ± 0.991          | 0.003*         |
| NIC <sub>2</sub> VP            | 3.450 ± 0.980         | 5.481 ± 1.054          | <0.001**       |

\* $P < 0.05$ , \*\* $P < 0.001$ ; NIC<sub>1</sub>, normalized iodine concentration of the initial tumor; NIC<sub>2</sub>, normalized iodine concentration of the adipose tissue around the rectal tumor; AP, arterial phase; VP, venous phase; LVI+, lymphovascular invasion positive; LVI-, lymphovascular invasion negative; BMI, body mass index; SD, standard deviation.

**Table 3.** T-staging of rectal cancer using preoperative conventional computed tomography and dual-energy computed tomography compared with postoperative histology staging

| Confusion matrix        |                 | Conventional CT |                | DECT arterial phase |                | DECT venous phase |                | Total |
|-------------------------|-----------------|-----------------|----------------|---------------------|----------------|-------------------|----------------|-------|
|                         |                 | T1-2            | T3-4a          | T1-2                | T3-4a          | T1-2              | T3-4a          |       |
| <b>Histologic stage</b> | Group C (T1-2)  | 11              | 7 <sup>a</sup> | 14                  | 4 <sup>a</sup> | 15                | 3 <sup>a</sup> | 18    |
|                         | Group D (T3-4a) | 9 <sup>b</sup>  | 22             | 4 <sup>b</sup>      | 27             | 2 <sup>b</sup>    | 29             | 31    |

<sup>a</sup>Seven patients with RC in group C were misdiagnosed as group D using conventional CT; 5 of them were corrected using DECT in the arterial phase (AP), and 6 of them were corrected using DECT in the venous phase (VP). In addition, the conventional CT diagnosis of 2 patients in group C was correct, but the DECT was misdiagnosed as group D. <sup>b</sup>Nine patients with RC in group D were misdiagnosed as group C using conventional CT; 6 of them were corrected using DECT in the AP, and 8 of them were corrected using DECT in the VP. In addition, the conventional CT diagnosis of 1 patient in group D was correct, but the DECT led to a misdiagnosis as group C. CT, computed tomography; DECT, dual-energy computed tomography; RC, rectal cancer.

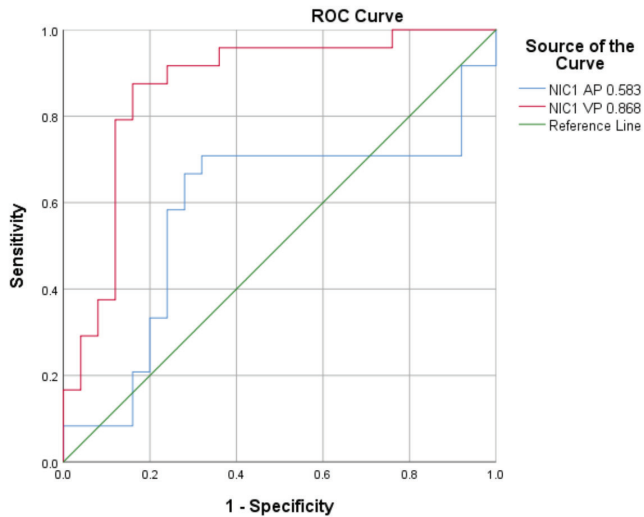


**Figure 4.** The receiver operating characteristic (ROC) curve showed the ability of preoperative normalized iodine concentration (NIC) values in the arterial phase (AP) and venous phase (VP) to predict the lymphovascular invasion (LVI) of rectal cancer. The ROC curves showed that the NIC<sub>1</sub> could predict the LVI of rectal cancer more accurately in the VP than in the AP. NIC<sub>1</sub>, normalized iodine concentration of initial tumor; NIC<sub>2</sub>, normalized iodine concentration of adipose tissue around rectal tumor.

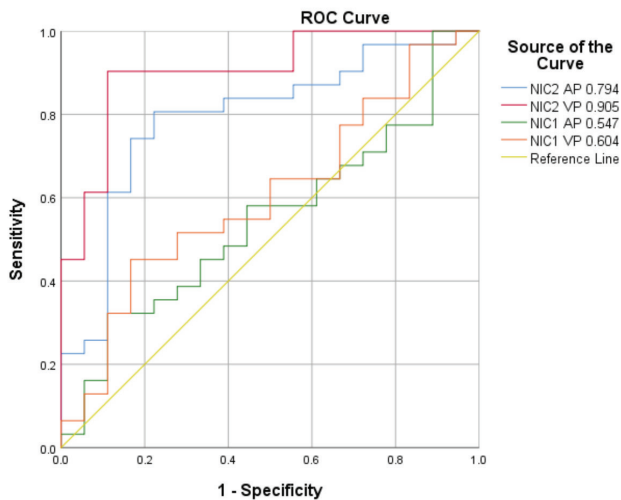


**Figure 5.** The receiver operating characteristic (ROC) curve showed the ability of preoperative normalized iodine concentration (NIC) values in the arterial phase (AP) and venous phase (VP) to predict the invasion of adipose tissue around the tumor; NIC<sub>1</sub> means the NIC of tumor tissue, and NIC<sub>2</sub> means the NIC of perirectal adipose tissue. The ROC curves showed that NIC<sub>2</sub> could predict the invasion of adipose tissue around the tumor more accurately in the VP than in the AP. NIC<sub>1</sub>, normalized iodine concentration of initial tumor; NIC<sub>2</sub>, normalized iodine concentration of adipose tissue around rectal tumor.

method for predicting LVI and improving the accuracy of preoperative RC T-staging.

Peng et al.<sup>33</sup> utilized the novel multiparametric imaging capabilities of DECT to predict very early distant metastasis (VEDM) following colorectal cancer surgery and noted that the venous enhancement fraction, the slope of the VP spectral curve ( $\lambda_{VP}$ ) and the inverse of the VP-standardized IC ( $1/NIC_{VP}$ ) presented significant discriminative abilities in predicting VEDM, with AUC values of 0.822, 0.738, and 0.713, respectively.

LVI is an early sign of lymph node metastasis and distant metastasis, which is the initial manifestation of lymph node metastasis and other types of organ metastasis;<sup>34</sup> the IC parameter of the tumor was applied in the prediction of LVI with an accuracy of 85.7%. Thus, it can guide clinical treatment and intervention in a relatively precise manner and in the early disease stage.

Jia et al.<sup>35</sup> compared the image quality of MRI and DECT virtual monochrome imaging techniques and assessed their accuracy

in T-staging, demonstrating that the overall diagnostic accuracy of dual-layer spectral CT and high-resolution MRI in T-staging was 65.67% and 71.64%, respectively, with no significant difference ( $P > 0.05$ ). Qin et al.<sup>36</sup> investigated the optimal DECT parameter-AP  $\lambda_{HU}$  for differentiating between T3 and T4a stages of RC, with an overall accuracy of 76.9%. The present study on the T-staging of RC was conducted according to different clinical treatment modalities and focused on distinguishing the difference between T1-2 and T3-4a, which was more relevant to clinical needs than the other studies. The authors of the present study comprehensively considered the critical factors for the selection of clinical treatment options, including both tumor T-staging and LVI. This study set the research protocol according to clinical needs; the diversity and depth of this study contribute to a more comprehensive understanding of the application of DECT in oncology and may lead to the development of future diagnostic and therapeutic strategies. With the continuous development of DECT technology and the growing demand for a more accurate prediction of cancer staging and metastasis in clinical practice, more spectral parameters may be derived<sup>33,37</sup> and combined with clinical parameters<sup>38</sup> or even radiomics and artificial intelligence<sup>37</sup> to further improve the predictive potential. This provides new opportunities for follow-up studies.

This study has several limitations. First, the number of patients was limited, and the study used an experimental methodology. In the future, performing a larger-scale and more accurate patient selection study to affirm the results would be worthwhile. Second, the type of all involved tumors was rectal adenocarcinoma, and whether other types of rectal tumors can be staged using this method should be verified in future. Third, the placement of ROI was subjective and could only avoid obvious large blood vessels; however, interaction with some small vessels may have caused inflammation of connective tissue, increasing the false positive rate of the study. Fourth, this study did not measure other quantitative parameters of DECT. A combination of other DECT parameters could enhance the accuracy of predicting the pathological indicators of RC. Fifth, the present study did not measure the size of the primary tumor or locate the position of the tumor, especially the accurate location of the supra- or sub-peritoneal layer, which are critical factors for the RC treatment plan. Sixth, comparisons between DECT and

other imaging techniques, such as MRI and TRUS, were not performed. Finally, this study was a single-center study and did not involve samples from other medical centers. Therefore, a complicated analysis using DECT parameters will be performed in future studies.

In conclusion, this study found that the quantitative determination of NIC in tumors can predict LVI. Furthermore, NIC in PAT via DECT can accurately, sensitively, and specifically distinguish whether serosa invasion has occurred in RC. In addition, the study first utilized NIC to evaluate the invasion of PAT and effectively reduce the difference of individual factors among patients. The DECT quantitative IC measurement was a useful clinical tool for the preoperative prediction of pathological indicators of RC.

### Conflict of interest disclosure

The authors declared no conflicts of interest.

### Funding

This work was supported by the Technology Development Plan of Shandong Province (grant number: 2014GSF118091) and the Shandong Medical and Health Science and Technology Development Plan (grant number: 2017WS715).

### References

1. Siegel RL, Miller KD, Fuchs HE, Jemal A. Cancer statistics, 2022. *CA Cancer J Clin*. 2022;72(1):7-33. [\[Crossref\]](#)
2. Burt JR, Waltz J, Ramirez A, et al. Predictive value of initial imaging and staging with long-term outcomes in young adults diagnosed with colorectal cancer. *Abdom Radiol (NY)*. 2021;46(3):909-918. [\[Crossref\]](#)
3. Amin MB, Greene FL, Edge SB, et al. The Eighth Edition AJCC Cancer Staging Manual: Continuing to build a bridge from a population-based to a more "personalized" approach to cancer staging. *CA Cancer J Clin*. 2017;67(2):93-99. [\[Crossref\]](#)
4. Foxtrot Collaborative Group. Feasibility of preoperative chemotherapy for locally advanced, operable colon cancer: the pilot phase of a randomised controlled trial. *Lancet Oncol*. 2012;13(11):1152-1160. [\[Crossref\]](#)
5. Monson JR, Weiser MR, Buie WD, et al. Practice parameters for the management of rectal cancer (revised). *Dis Colon Rectum*. 2013;56(5):535-550. [\[Crossref\]](#)
6. Nicum S, Midgley R, Kerr DJ. Colorectal cancer. *Acta Oncol*. 2003;42(4):263-275. [\[Crossref\]](#)
7. Le DT, Kim TW, Van Cutsem E, et al. Phase II open-label study of pembrolizumab in treatment-refractory, microsatellite instability-high/mismatch repair-deficient metastatic colorectal cancer: KEYNOTE-164. *J Clin Oncol*. 2020;38(1):11-19. [\[Crossref\]](#)
8. Opara CO, Khan FY, Kabiraj DG, Kauser H, Palakeel JJ, Ali M, Chaduvula P, Chhabra S, Lamsal Lamichhane S, Ramesh V, Mohammed L. The value of magnetic resonance imaging and endorectal ultrasound for the accurate preoperative T-staging of rectal cancer. *Cureus*. 2022;14(10):e30499. [\[Crossref\]](#)
9. Xia Q, Cheng W, Bi J, Ren AP, Chen X, Li T. Value of biplane transrectal ultrasonography plus micro-flow imaging in preoperative T staging and rectal cancer diagnosis in combination with CEA/CA199 and MRI. *BMC Cancer*. 2023;23(1):860. [\[Crossref\]](#)
10. Boot J, Gomez-Munoz F, Beets-Tan RGH. Imaging of rectal cancer. *Radiologe*. 2019;59(Suppl 1):46-50. [\[Crossref\]](#)
11. Beets-Tan RG, Beets GL. Rectal cancer: review with emphasis on MR imaging. *Radiology*. 2004;232(2):335-346. [\[Crossref\]](#)
12. Horvat N, Carlos Tavares Rocha C, Clemente Oliveira B, Petkovska I, Gollub MJ. MRI of Rectal Cancer: Tumor Staging, Imaging Techniques, and Management. *Radiographics*. 2019;39(2):367-387. [\[Crossref\]](#)
13. Napp AE, Enders J, Roehle R, et al. Analysis and prediction of claustrophobia during MR imaging with the claustrophobia questionnaire: an observational prospective 18-month single-center study of 6500 patients. *Radiology*. 2017;283(1):148-157. [\[Crossref\]](#)
14. Kijima S, Sasaki T, Nagata K, Utano K, Lefor AT, Sugimoto H. Preoperative evaluation of colorectal cancer using CT colonography, MRI, and PET/CT. *World J Gastroenterol*. 2014;20(45):16964-16975. [\[Crossref\]](#)
15. Xu JJ, Taudorf M, Ulriksen PS, et al. Gastrointestinal applications of iodine quantification using dual-energy CT: a systematic review. *Diagnostics (Basel)*. 2020;10(10):814. [\[Crossref\]](#)
16. Karcaaltincaba M, Karaosmanoglu D, Akata D, Sentürk S, Ozmen M, Alibek S. Dual energy virtual CT colonoscopy with dual source computed tomography: initial experience. *Rofo*. 2009;181(9):859-862. [\[Crossref\]](#)
17. Kang HJ, Kim SH, Bae JS, Jeon SK, Han JK. Can quantitative iodine parameters on DECT replace perfusion CT parameters in colorectal cancers? *Eur Radiol*. 2018;28(11):4775-4782. [\[Crossref\]](#)
18. Ascenti G, Mazziotti S, Lamberto S, et al. Dual-energy CT for detection of endoleaks after endovascular abdominal aneurysm repair: usefulness of colored iodine overlay. *AJR Am J Roentgenol*. 2011;196(6):1408-1414. [\[Crossref\]](#)
19. Chuang-Bo Y, Tai-Ping H, Hai-Feng D, et al. Quantitative assessment of the degree of differentiation in colon cancer with dual-energy spectral CT. *Abdom Radiol (NY)*. 2017;42(11):2591-2596. [\[Crossref\]](#)
20. Yang L, Shi G, Zhou T, Li Y, Li Y. Quantification of the iodine content of perigastric adipose tissue by dual-energy CT: a novel method for preoperative diagnosis of T4-stage gastric cancer. *PLoS One*. 2015;10(9):e0136871. [\[Crossref\]](#)
21. Kato T, Uehara K, Ishigaki S, et al. Clinical significance of dual-energy CT-derived iodine quantification in the diagnosis of metastatic LN in colorectal cancer. *Eur J Surg Oncol*. 2015;41(11):1464-1470. [\[Crossref\]](#)
22. Wang D, Zhuang Z, Wu S, et al. A dual-energy CT radiomics of the regional largest short-axis lymph node can improve the prediction of lymph node metastasis in patients with rectal cancer. *Front Oncol*. 2022;12:846840. [\[Crossref\]](#)
23. Altenbernd J, Forsting M, Lauenstein T, Wetter A. Improved image quality and detectability of hypovascular liver metastases on DECT with different adjusted window settings. *Rofo*. 2017;189(3):228-232. [\[Crossref\]](#)
24. Lenga L, Czwikla R, Wichmann JL, et al. Dual-energy CT in patients with colorectal cancer: Improved assessment of hypoattenuating liver metastases using noise-optimized virtual monoenergetic imaging. *Eur J Radiol*. 2018;106:184-191. [\[Crossref\]](#)
25. Ratajczak P, Serafin Z, Sławińska A, Słupski M, Leszczyński W. Improved imaging of colorectal liver metastases using single-source, fast kVp-switching, dual-energy CT: preliminary results. *Pol J Radiol*. 2018;83:e643-e649. [\[Crossref\]](#)
26. Al-Najami I, Lahaye MJ, Beets-Tan RGH, Baatrup G. Dual-energy CT can detect malignant lymph nodes in rectal cancer. *Eur J Radiol*. 2017;90:81-88. [\[Crossref\]](#)
27. Li Y, Li X, Ren X, Ye Z. Assessment of the aggressiveness of rectal cancer using quantitative parameters derived from dual-energy computed tomography. *Clin Imaging*. 2020;68:136-142. [\[Crossref\]](#)
28. Zhou X, Yi Y, Liu Z, et al. Radiomics-based preoperative prediction of lymph node status following neoadjuvant therapy in locally advanced rectal cancer. *Front Oncol*. 2020;10:604. [\[Crossref\]](#)
29. Lim SB, Yu CS, Jang SJ, Kim TW, Kim JH, Kim JC. Prognostic significance of lymphovascular invasion in sporadic colorectal cancer. *Dis Colon Rectum*. 2010;53(4):377-384. [\[Crossref\]](#)
30. Stacker SA, Achen MG, Jussila L, Baldwin ME, Alitalo K. Lymphangiogenesis and cancer metastasis. *Nat Rev Cancer*. 2002;2(8):573-583. [\[Crossref\]](#)
31. Zhang Y, He K, Guo Y, et al. A novel multimodal radiomics model for preoperative prediction of lymphovascular invasion in rectal cancer. *Front Oncol*. 2020;10:457. [\[Crossref\]](#)
32. Wu ZJ, Hippe DS, Zamora DA, et al. Accuracy of dual-energy computed tomography

- techniques for fat quantification in comparison with magnetic resonance proton density fat fraction and single-energy computed tomography in an anthropomorphic phantom environment. *J Comput Assist Tomogr.* 2021;45(6):877-887. [\[Crossref\]](#)
33. Peng W, Wan L, Zhao R, et al. Novel biomarkers based on dual-energy computed tomography for risk stratification of very early distant metastasis in colorectal cancer after surgery. *Quant Imaging Med Surg.* 2024;14(1):618-632. [\[Crossref\]](#)
34. Wang X, Cao Y, Ding M, et al. Oncological and prognostic impact of lymphovascular invasion in Colorectal Cancer patients. *Int J Med Sci.* 2021;18(7):1721-1729. [\[Crossref\]](#)
35. Jia Z, Guo L, Yuan W, et al. Performance of dual-layer spectrum CT virtual monoenergetic images to assess early rectal adenocarcinoma T-stage: comparison with MR. *Insights Imaging.* 2024;15(1):11. [\[Crossref\]](#)
36. Qin M, Liu M, Huang R, et al. Preoperative T-staging of colorectal cancer by dual-energy computed tomography: a retrospective study. *Curr Med Imaging.* 2024;20:1-7. [\[Crossref\]](#)
37. Chen M, Jiang Y, Zhou X, Wu D, Xie Q. Dual-energy computed tomography in detecting and predicting lymph node metastasis in malignant tumor patients: a comprehensive review. *Diagnostics (Basel).* 2024;14(4):377. [\[Crossref\]](#)
38. Sato K, Morohashi H, Tsushima F, et al. Dual energy CT is useful for the prediction of mesenteric and lateral pelvic lymph node metastasis in rectal cancer. *Mol Clin Oncol.* 2019;10(6):625-630. [\[Crossref\]](#)